

Online Estimation of Power System Inertia Using Dynamic Regressor Extension and Mixing

Johannes Schiffer, Petros Aristidou and Romeo Ortega

Abstract—The increasing penetration of power-electronic-interfaced devices is expected to have a significant effect on the overall system inertia and a crucial impact on the system dynamics. In the future, the reduction of inertia will have drastic consequences on protection and real-time control and will play a crucial role in the system operation. Therefore, in a highly deregulated and uncertain environment, it is necessary for Transmission System Operators to be able to monitor the system inertia in real time. We address this problem by developing and validating an online inertia estimation algorithm. The estimator is derived using the recently proposed dynamic regressor extension and mixing procedure. The performance of the estimator is demonstrated via several test cases using the 1013-machine ENTSO-E dynamic model.

Index Terms—Power system inertia, power system dynamics, power system stability, low-inertia systems, parameter estimation.

I. INTRODUCTION

A. Motivation and Existing Literature

TRADITIONALLY, power systems have been relying on the inertia provided by synchronous generators to provide the necessary energy buffer for smoothing out sudden power imbalances (deficit or surplus) in the system. The inertia of conventional generators creates a direct physical connection to the grid, thus providing instantaneous power when necessary and helping to curb the frequency deviations created by abrupt power imbalances.

In modern power systems, conventional power plants are gradually being replaced by power-electronic(PE)-interfaced generators (mainly, integrating renewable energy sources) and high capacity network interconnections being implemented through high voltage direct current (HVDC) links. Consequently, the replacement of synchronous generators with PE-interfaced devices decreases the available inertia in the system and can lead to much faster frequency dynamics in the grid [1]–[4]. In this situation, the dynamic behavior can endanger the system by stressing the control and protection schemes, which were not designed to operate in such conditions [1], [2], leading to cascaded failures and disconnections. Moreover, the remaining legacy components could be endangered if they cannot withstand the emerging dynamics [1], [4].

In addition, in the present-day deregulated and uncertain environment, it becomes very difficult for Transmission Sys-

tem Operators (TSOs) to accurately track the system inertia and provide guarantees about the system stability [1], [3]. This inability leads to overly conservative operational planning scenarios, which inflate the operational costs. Hence, the capability to monitor the inertia available in the system in real time would allow TSOs to operate with lower security margins (and cost) by taking appropriate actions to secure the system operation.

Several techniques for power system inertia estimation have been proposed in the literature. The bulk amount of available inertia estimators are based on a simplified swing equation model and only work offline, *i.e.*, with data collected after an event [5]–[11]. While such *a posteriori* inertia estimation can be very useful, the information might arrive too late for any preventive or corrective actions to take place. In [7], PMU measurements are used to estimate regional inertia values and to then reconstruct the total inertia. The estimation relies on the accurate detection of a suitable event and requires post-processing the PMU data.

A near real-time, iterative, inertia estimation algorithm combining Least-Squares, Newton-Raphson and Modal Assurance Criterion techniques is proposed in [12]. In [13], [14] an online estimation algorithm is presented based on the linearized swing equation and a set of four filters implemented as sliding data windows. Yet, in addition to the active power flow also the rate of change, *i.e.*, the derivative, of the frequency at the generators needs to be known. Furthermore, the estimation method is only applicable immediately after a disturbance and critically depends on the exact knowledge of the time at which the disturbance occurs. To ensure the latter an additional disturbance time estimation algorithm is proposed in [14]. A statistical approach using steady-state and relatively small frequency variations is presented in [15]. The proposed online-estimation method in [16] requires the injection of an additional probing signal, which complicates its implementation.

B. Contributions

Our main contributions in this work are three-fold:

- 1) We propose an algorithm which allows to estimate in real time the inertia constant and the aggregated mechanical power setpoint of a large-scale power system. The algorithm is derived using a first-order nonlinear aggregated power system model in combination with the recently proposed dynamic regressor and mixing (DREM) procedure [17].
- 2) The performance of the estimator is demonstrated on a 1013-machine ENTSO-E test system with 21382 buses

J. Schiffer is with Brandenburgische Technische Universität Cottbus-Senftenberg, 03046 Cottbus, Germany (e-mail: schiffer@b-tu.de).

P. Aristidou is with University of Leeds, LS2 9JT Leeds, UK (e-mail: p.aristidou@leeds.ac.uk).

R. Ortega is with CNRS L2S, 91192 Gif Sur Yvette, France (e-mail: romeo.ortega@lss.supelec.fr).

and 133997 states, which is implemented in the dynamic simulation software RAMSES [18]. The considered scenarios consist of two generator outages and a rescheduling event. Neither the location nor the size of the perturbations need to be known and in all scenarios the same estimator gains are used. Furthermore, our proposed algorithm only requires frequency and electrical power measurements from primary-frequency-controlled (PFC) generators, which typically represent a subset of all machines in the system. As pointed out in [13], such data can be provided using synchronized measurement technology (SMT) [19].

- 3) We show that the PFC power injection signal can be well-approximated by a simple, aggregated model of the turbine-governor dynamics of the PFC units. Naturally, this leads to reduction of the required measurements and we illustrate that this approximation only results in a minor reduction of the achievable estimator accuracy.

The remainder of the paper is structured as follows. The aggregated power system model and the problem statement are introduced in Section II. The DREM-based inertia estimator is derived in Section III. The employed aggregated power system model is validated in Section IV using simulation results from a detailed dynamic 1013-machine ENTSO-E system obtained with the software RAMSES. Moreover the estimator is tested via a nominal outage scenario. The performance is investigated further in Section V with two additional test cases. Some final conclusions and a brief outlook on future work are given in Section VI.

II. AGGREGATED POWER SYSTEM MODEL AND PROBLEM FORMULATION

A. Center of Inertia Frequency Dynamics

For the purpose of deriving an online inertia estimator, we seek to represent the frequency dynamics of a primary-controlled power system using an equivalent reduced-order model. We assume that $N_{\text{PFC}} > 0$ is the number of PFC generators in the system and $N_{\text{unc}} \geq 0$ is the number of generators (and large motors) without PFC. Thus, $N = N_{\text{PFC}} + N_{\text{unc}}$ is the total number of generators (and large motors) in the system. It is well-known [3], [20], [21] that the principal frequency dynamics of a power system can be described by the evolution of the center of inertia (COI) speed, which is defined as

$$\omega_{\text{COI}} = \frac{\sum_{i=1}^N H_i \omega_i}{\sum_{i=1}^N H_i}. \quad (1)$$

Here, $\omega_i : \mathbb{R}_{\geq 0} \rightarrow \mathbb{R}_{> 0}$ is the angular frequency of the rotor of the i -th unit and $H_i \in \mathbb{R}_{> 0}$ the i -th unit's inertia constant¹.

Let $S_{B_i} \in \mathbb{R}_{> 0}$ denote the power rating of the i -th unit and $P_{m_i} \in \mathbb{R}$ its scheduled (constant) mechanical power. Then

$$S_B = \sum_{i=1}^N S_{B_i}$$

¹The sets $\mathbb{R}_{\geq 0}$ and $\mathbb{R}_{> 0}$ denote the non-negative and positive real numbers, respectively. Hence, the notation $\omega_i : \mathbb{R}_{\geq 0} \rightarrow \mathbb{R}_{> 0}$ means that $\omega_i(t)$ is a function, which takes positive values for all times $t \in \mathbb{R}_{\geq 0}$.

represents the total power rating of the considered system. Furthermore, the total inertia constant of the power system is given by

$$H_{\text{tot}} = \frac{\sum_{i=1}^N H_i S_{B_i}}{\sum_{i=1}^N S_{B_i}}$$

Likewise, the total mechanical power is given by

$$P_{m,\text{tot}} = P_{m,\text{PFC}} + P_{m,\text{unc}} = \sum_{i=1}^{N_{\text{PFC}}} P_{m_i} + \sum_{i=1}^{N_{\text{unc}}} P_{m_i}. \quad (2)$$

Let $P_{e,\text{PFC}} : \mathbb{R}_{\geq 0} \rightarrow \mathbb{R}_{\geq 0}$ denote the aggregated generated electrical power by the PFC generators and $P_{e,\text{unc}} : \mathbb{R}_{\geq 0} \rightarrow \mathbb{R}_{\geq 0}$ that by the non-PFC units. Then, the total generated electrical power is denoted by $P_{e,\text{tot}} : \mathbb{R}_{\geq 0} \rightarrow \mathbb{R}_{\geq 0}$ and satisfies

$$P_{e,\text{tot}} = P_{e,\text{PFC}} + P_{e,\text{unc}} = P_{\text{load}} + P_{\text{loss}} - P_{\text{ren}}, \quad (3)$$

where $P_{\text{load}} : \mathbb{R}_{\geq 0} \rightarrow \mathbb{R}_{\geq 0}$ is the total load demand in the system, $P_{\text{loss}} : \mathbb{R}_{\geq 0} \rightarrow \mathbb{R}_{\geq 0}$ are the total losses and $P_{\text{ren}} : \mathbb{R}_{\geq 0} \rightarrow \mathbb{R}_{\geq 0}$ is the total renewable generation power.

With these considerations, the principal frequency dynamics of the system can be described by the aggregated swing equation [20]

$$\dot{\omega}_{\text{COI}} = \frac{\omega_0^2}{2H_{\text{tot}}S_B} \frac{\Delta P}{\omega_{\text{COI}}} = \frac{\omega_0^2}{2H_{\text{tot}}S_B} \left(\frac{P_{m,\text{tot}} + P_{\text{PFC,tot}} - P_{e,\text{tot}}}{\omega_{\text{COI}}} \right), \quad (4)$$

where $\omega_0 \in \mathbb{R}_{> 0}$ is the nominal network frequency and $P_{\text{PFC,tot}} : \mathbb{R}_{\geq 0} \rightarrow \mathbb{R}_{\geq 0}$ is the total PFC power injection².

B. Problem Formulation

Determining directly the variables ω_{COI} , $P_{m,\text{tot}}$ and $P_{e,\text{tot}}$ in (4) is very hard in practice. Hence, any real-time inertia estimator based on (4) would not be implementable. However, modern power systems are equipped with advanced SMTs or wide-area measurement systems (WAMS) [19] that can provide a TSO access to the measurements of the PFC units. Using these measurements, we can approximate equation (4) describing the COI frequency dynamics by expressing the power balance ΔP on the right hand-side with information from the PFC generators, *i.e.*,

$$\Delta P = P_{m,\text{PFC}} + P_{\text{PFC,tot}} - P_{e,\text{PFC}},$$

where from (3)

$$P_{e,\text{PFC}} = -P_{e,\text{unc}} + P_{\text{load}} + P_{\text{loss}} - P_{\text{ren}}. \quad (5)$$

In addition, the COI frequency is approximated by the average frequency of the PFC units, *i.e.*,

$$\omega_{\text{av}} = \frac{\sum_{i=1}^{N_{\text{PFC}}} \omega_i}{N_{\text{PFC}}}.$$

These steps yield the following approximation of the COI frequency dynamics (4)

$$\dot{\omega}_{\text{av}} = \frac{\omega_0^2}{2H_{\text{tot}}S_B} \left(\frac{P_{m,\text{PFC}} + P_{\text{PFC,tot}} - P_{e,\text{PFC}}}{\omega_{\text{av}}} \right), \quad (6)$$

²For the purpose of inertia estimation, we are interested in fast time scales. Therefore secondary control actions are neglected in the torque balance (4).

which is used in the remainder of this work.

Furthermore, the above discussion on the available measurements is summarized in the following assumption³.

Assumption 2.1: The signals ω_{av} , $P_{PFC,tot}$ and $P_{e,PFC}$ are measurable.

If information on the type and parameters of the turbine-governor systems is available, $P_{PFC,tot}$ can be obtained from the average frequency ω_{av} . Then, Assumption 2.1 can be further relaxed. This is demonstrated in Section IV for the ENTSO-E 1013-machine system.

We are interested in the following problem.

Problem 2.2: Consider the system (6) with measurable signals ω_{av} , $P_{PFC,tot}$ and $P_{e,PFC}$. Identify the parameters H_{tot} and $P_{m,PFC}$.

We remark that, as in (4), the parameter H_{tot} is the *total* inertia constant of PFC and non-PFC units. Hence, we seek to estimate the total system inertia using only partial system information from the PFC units. In addition, the total mechanical power $P_{m,PFC}$ should be estimated. This is useful in case any frequency variations are caused by changes in $P_{m,PFC}$, e.g., due to rescheduling or an outage of a PFC generator.

III. SYSTEM PARAMETRIZATION, REGRESSION CONSTRUCTION AND DREM ESTIMATOR

A. System Parametrization

We begin our exposition by bringing the model (6) in the standard form for dynamic parameter estimation schemes [22]–[24]. First, we define the new variables

$$y = \omega_{av}, \quad x = P_{PFC,tot}, \quad u = P_{e,PFC},$$

the constant

$$b_1 = \frac{\omega_0^2}{2S_B},$$

and the parameters

$$\eta_1 = \frac{1}{H_{tot}}, \quad \eta_2 = \frac{P_{m,PFC}}{H_{tot}}. \quad (7)$$

Then, (6) takes the form

$$\dot{y} = \eta_1 b_1 \left(\frac{x-u}{y} \right) + \eta_2 \frac{b_1}{y}. \quad (8)$$

This system parametrization is used for the regression construction and estimator development detailed below.

B. Regression Construction

To address Problem 2.2, we construct a regression by using the dynamics described by (8). Let

$$p = \frac{d}{dt}$$

denote a differentiation operator. Then, by applying the operator $\frac{\alpha p}{(p+\alpha)}$ with some $\alpha > 0$ to (8), we obtain

$$\frac{\alpha p}{(p+\alpha)} y = \eta_1 \frac{\alpha}{(p+\alpha)} b_1 \left(\frac{x-u}{y} \right) + \eta_2 \frac{\alpha}{(p+\alpha)} \frac{b_1}{y} + \epsilon, \quad (9)$$

³As long as the data is time-stamped it does not have to arrive in real time to execute the estimation algorithm, since the execution can also be shifted in time, giving a slightly delayed estimation.

where ϵ is an exponentially decaying term stemming from the filters' initial conditions. Then, by setting

$$\xi_1 = \frac{\alpha p}{(p+\alpha)} y, \quad \xi_2 = \frac{\alpha}{(p+\alpha)} b_1 \left(\frac{x-u}{y} \right), \quad \xi_3 = \frac{\alpha}{(p+\alpha)} \frac{b_1}{y}.$$

we can rewrite (9) compactly as

$$\xi_1 = \eta_1 \xi_2 + \eta_2 \xi_3 + \epsilon,$$

or, equivalently,

$$z = \phi^\top \eta + \epsilon, \quad (10)$$

with

$$z = \xi_1, \quad \phi^\top = [\xi_2 \quad \xi_3], \quad \eta^\top = [\eta_1 \quad \eta_2].$$

C. DREM Parameter Estimator

To construct a parameter estimator for the regressor equation (10), we follow the DREM procedure [17]. The regression (10) is of dimension 1, but the number of unknown parameters is $q = 2$. Hence, the first step of the DREM procedure is to introduce a linear, \mathcal{L}_∞ -stable operator $\mathcal{H} : \mathcal{L}_\infty \rightarrow \mathcal{L}_\infty$, the output of which may be decomposed for any bounded input as

$$(\cdot)_f(t) = [\mathcal{H}(\cdot)](t) + \epsilon_t,$$

where ϵ_t is an exponentially decaying term. This operator can be chosen in several ways. For instance, a possible choice would be an exponentially stable linear time-invariant (LTI) filter of the form

$$\mathcal{H}(p) = \frac{\alpha}{p+\alpha}, \quad \alpha \neq 0.$$

Another option is to choose a delay operator, i.e.,

$$[\mathcal{H}(\cdot)](t) = (\cdot)(t-d), \quad (11)$$

for some $d > 0$. The impact of different operators on the transient performance of the DREM estimator is extensively discussed in [17], [25]. In the authors' experience the delay operator (11) has proven very successful in power engineering applications. Therefore, this option is also chosen for the present application.

In the second step, we apply the operator (11) to the regressor (10). This yields the filtered regression⁴

$$z_f = \phi_f^\top \eta, \quad (12)$$

which in the present case is equivalent to

$$z(t-d) = \phi^\top(t-d)\eta.$$

The third step in DREM consists of piling up the original regressor (10) with the filtered regressor (12), which gives the extended regressor system

$$\begin{bmatrix} z \\ z_f \end{bmatrix} = \Phi \eta, \quad (13)$$

⁴To simplify the presentation in the sequel we neglect the ϵ and ϵ_t terms, see also [17].

where

$$\Phi = \begin{bmatrix} \phi^T \\ \phi_f^T \end{bmatrix}. \quad (14)$$

Next, we have that

$$\text{adj}(\Phi)\Phi = \Delta I_2,$$

where I_2 denotes the 2×2 identity matrix and

$$\Delta = \det(\Phi). \quad (15)$$

Consequently, by premultiplying (13) with the adjunct matrix of Φ we obtain two scalar regressors

$$\mathcal{Z} = \begin{bmatrix} \mathcal{Z}_1 \\ \mathcal{Z}_2 \end{bmatrix} = \Delta \eta, \quad (16)$$

where

$$\mathcal{Z} = \text{adj}(\Phi) \begin{bmatrix} z \\ z_f \end{bmatrix}.$$

We define $\hat{\eta}$ as the estimated value of the parameter vector η . By using the decoupled regression (16), we can then estimate η via the gradient algorithm

$$\begin{aligned} \dot{\hat{\eta}}_1 &= \gamma_1 \Delta (\mathcal{Z}_1 - \Delta \hat{\eta}_1), \\ \dot{\hat{\eta}}_2 &= \gamma_2 \Delta (\mathcal{Z}_2 - \Delta \hat{\eta}_2), \end{aligned} \quad (17)$$

where $\gamma_1 > 0$ and $\gamma_2 > 0$ are tuning gains. A block-diagram of the proposed estimator is shown in Fig. 1.

Recall that a signal $\xi : \mathbb{R}_{\geq 0} \rightarrow \mathbb{R}^m$ is in \mathcal{L}_2 if its \mathcal{L}_2 -norm $\|\xi\|_{\mathcal{L}_2}$, given by

$$\|\xi\|_{\mathcal{L}_2} = \sqrt{\int_0^\infty \xi^\top(t)\xi(t)dt},$$

is finite. Introducing the error coordinates $\tilde{\eta} = \hat{\eta} - \eta$ and using (16), the error dynamics corresponding to (17) are given by

$$\dot{\tilde{\eta}} = -\text{diag}(\gamma_1, \gamma_2)\Delta^2\tilde{\eta}, \quad (18)$$

where $\text{diag}(\cdot)$ denotes a diagonal matrix. Hence, we see that the following equivalence holds

$$\lim_{t \rightarrow \infty} \tilde{\eta} = 0 \quad \Leftrightarrow \quad \Delta \notin \mathcal{L}_2. \quad (19)$$

Note that the requirement (19) is different from that in conventional parameter identification techniques. The usual persistency of excitation (PE) condition is defined as [22]–[24]

$$\int_t^{t+\tau} \phi(s)\phi^\top(s)ds \geq \delta I_2,$$

for some $\tau > 0$ and δ . Hence, PE is a property of the regressor ϕ , while DREM requires the determinant of the matrix Φ not to be square integrable. We refer to [17], [25] for an in-depth analysis of the convergence and robustness properties of DREM parameter estimators as well as for examples of regressors, which are not PE but satisfy $\Delta \notin \mathcal{L}_2$.

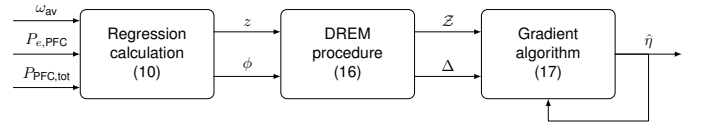


Fig. 1: Block diagram of the DREM-based online inertia estimator.

IV. NUMERICAL VERIFICATION ON 1013-MACHINE ENTSO-E SYSTEM: NOMINAL TEST CASE

The performance of the proposed inertia DREM estimator is evaluated on the ENTSO-E system with topology and parameters as detailed in [26]. The system has a total of 21382 buses and $N = 1013$ synchronous generators. Out of these, PFC units are connected at $N_{\text{PFC}} = 871$ buses, while the generators at the remaining $N_{\text{unc}} = N - N_{\text{PFC}}$ buses have a constant active power setpoint. The AVR, governor, and PSS models of the PFC units are modeled each as detailed in [26] and its references. The full detailed model consists of 133997 differential-algebraic states.

The performance evaluation is undertaken as follows. At first, we demonstrate that the main frequency dynamics of the 1013-machine ENTSO-E system can indeed be captured by the model (6). In addition, we show that for our selected benchmark system the PFC power injection $P_{\text{PFC,tot}}$ can be well-approximated using an aggregated, simple, model of the turbine-governor dynamics of the PFC units.

After this model validation step, we employ the DREM estimator (17) to identify the overall inertia constant of the 1013-machine ENTSO-E system. The time-domain response of the system is obtained using the dynamic simulation software RAMSES [18].

A. Aggregated Power System Model Including Turbine-Governor Dynamics of Primary-Controlled Units

The majority of power plants in the considered ENTSO-E test system are thermal power plants. Therefore, similarly to [21], we assume that the turbine dynamics of the aggregated primary-controlled power plants can be represented by the TGOV1 model [27]

$$P_{\text{PFC,tot}} = \frac{1 + pT_z}{1 + pT_p} (-K_P(\omega_{\text{av}} - \omega_0)), \quad (20)$$

where $K_P \in \mathbb{R}_{>0}$ is the total primary (droop) control gain and $T_z \in \mathbb{R}_{>0}$ as well as $T_p \in \mathbb{R}_{>0}$ are time constants of the turbine-governor system of the aggregated generators⁵.

Thus, the overall aggregated power system dynamics are given by (6) and (20) and the corresponding system parameters for the aggregated ENTSO-E system are given in Table I.

Remark 4.1: As indicated in [21], the model (20) has proven to be sufficiently accurate for representing PFC effects provided predominantly by steam power plants. If a significant amount of other units, such as hydro or gas power plants, also contribute to PFC, then the model (20) should be modified to account for these dynamics. Since we are mainly concerned

⁵We recall that $p = \frac{d}{dt}$ is a differentiation operator.

TABLE I: Aggregated ENTSO-E system parameters

Parameter	Value
S_B	570.892 [GW]
H_{tot}	3.665 [s]
ω_0	1.000 [rad s ⁻¹]
K_P	2.495 [pu]
P_m	0.498 [pu]
T_p	12.983 [s]
T_z	6.000 [s]

with inertia estimation (and the dynamics (6) are independent of the PFC mix), we leave this extension for future research.

B. Validation of Aggregated Model

To validate the aggregated reduced-order model (6), (20), we first run a simulation of an outage of a power plant (the PFC unit 'FR918226' in France with $S_{B_{645}} = 1755$ MW and $P_{m,645} = 1455$ MW) in the bulk power system model using RAMSES. Then, we compute the aggregated data and parameters as defined in Section II-A. After that, we use the variables $P_{e,\text{tot}}$ and $P_{m,\text{tot}}$ as inputs to the aggregated model (6), (20) and run a simulation of the aggregated model in Matlab/Simulink. Finally, the average frequency f_{av} and total PFC injections $P_{\text{PFC,tot}}$ obtained with both models are compared. This comparison is illustrated in Fig. 2a and Fig. 2b.

These results show that the aggregated reduced-order model (6), (20) offers a good approximation of the full-order ENTSO-E model. A small discrepancy at the frequency nadir can be explained by the fact that the non-PFC units are not explicitly considered in the model (6), (20). Therefore, we conclude that using the model (6) for the online-inertia estimator design is admissible. Likewise, the turbine-governor model (20) provides a good approximation of the PFC power injection $P_{\text{PFC,tot}}$.

C. Online-Inertia Estimation: Nominal Test Scenario

The DREM-based estimator (17), see also Fig. 1, is implemented in Matlab/Simulink. The estimator parameters are chosen as:

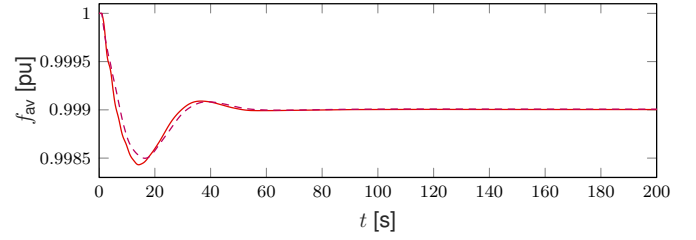
$$\alpha = 10^3, \quad d = 2, \quad \gamma_1 = \gamma_2 = 10^{10}.$$

This is motivated as follows. The operator used in (9) should not remove any important information from the filtered signals. Furthermore, the inertia constant mainly impacts the first few seconds of the power system's response to a disturbance. Hence, the choice $d = 2$ s. Finally, the values for the gains γ_1 and γ_2 have been tuned, such that the estimator possesses satisfactorily convergence properties for the ENTSO-E system under study.

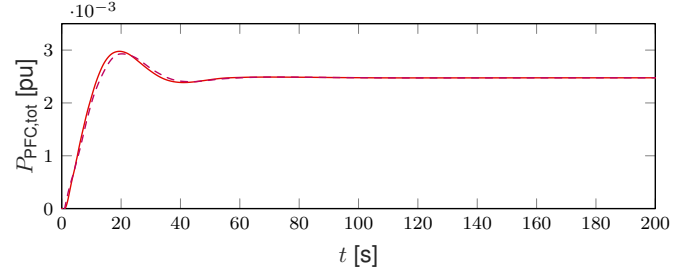
For the considered test system we work in per unit values. Hence, the system base S_B is removed from (6). Moreover, we find from Table I the nominal parameter values (see also (7))

$$\eta_1 = \frac{1}{H_{\text{tot}}} = 0.273, \quad \eta_2 = \frac{P_{m,\text{PFC}}}{H_{\text{tot}}} = 0.136.$$

The performance of our proposed estimator is illustrated for the considered test case in Fig. 3a with initial condition



(a) Comparison of the average electrical frequency f_{av}



(b) Comparison of the PFC power injection $P_{\text{PFC,tot}}$

Fig. 2: Comparison of the average electrical frequency f_{av} and the PFC power injection $P_{\text{PFC,tot}}$ obtained from the bulk ENTSO-E system ('-') and from the aggregated model (6), (20) ('- -').

$\hat{\eta}(0) = \text{diag}(0.3, 0.2)\eta$. It can be observed that, after some initial transients, the estimates $\hat{\eta}$ converge to constant values. This can also be appreciated from the trajectories in Fig. 3b, which show the evolution of the relative errors $\frac{\hat{\eta}_i}{\eta_i}$, $i = 1, 2$. The final estimates are

$$\hat{\eta}_1^s = 0.290, \quad \hat{\eta}_2^s = 0.145,$$

or, expressed in relative terms,

$$\frac{\hat{\eta}_1^s}{\eta_1} = 1.064, \quad \frac{\hat{\eta}_2^s}{\eta_2} = 1.064.$$

Hence, the final estimation error is below 7%. In further numerical experiments we have observed a very similar behavior for a large variety of other initial conditions $\hat{\eta}(0) = \text{diag}(\alpha_1, \alpha_2)\eta$ with $\alpha_i \in [0, 30]$, $i = 1, 2$.

To assess the impact of the error introduced when using the model (20), we take the measurement of $P_{\text{PFC,tot}}$ from the simulation and feed it directly as input to the estimator (17) instead of using the model (20). Doing so yields a stationary estimation error of only 1%. Hence, as one would expect, while the use of the model (20) reduces the number of required measurements, this is done at the expense of a (slightly) higher estimation error (7% instead of 1%). Furthermore, these experiments show that the approximations made in the derivation of the aggregated model (6) and the use of only data from PFC units (see Section II) does not have significant effect on the estimation accuracy.

As can be seen from (18), the fact that $\Delta \notin \mathcal{L}_2$ with Δ given in (15) is crucial for the performance of the inertia estimator (17). Since the numerical experiments are conducted on a finite

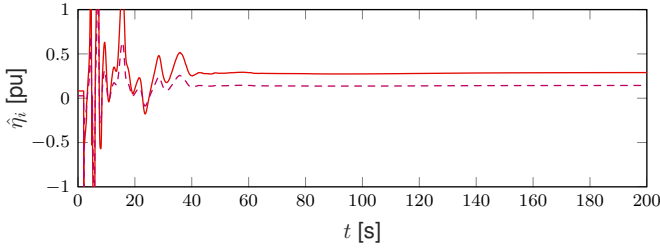
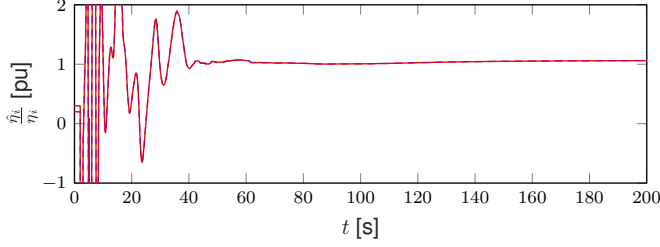
(a) Trajectories of the parameter estimates $\hat{\eta}$ (b) Trajectories of the parameter estimates $\hat{\eta}$ relative to the nominal parameter values η

Fig. 3: Absolute and relative trajectories of the parameter estimates $\hat{\eta}_i$, respectively $\frac{\hat{\eta}_i}{\eta_i}$ ($i = 1$ ‘-’ and $i = 2$ ‘- -’) with initial condition $\hat{\eta}(0) = \text{diag}(0.3, 0.2)\eta$.

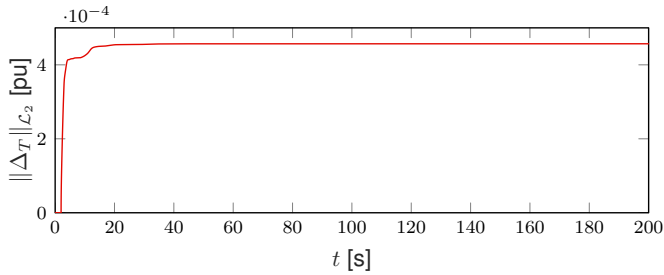


Fig. 4: Evolution of the truncated L_2 -norm $\|\Delta_T\|_{\mathcal{L}_2} = \sqrt{\int_0^T \Delta^2 d\tau}$ of Δ defined in (15).

time-horizon, we investigate the behavior of the truncated \mathcal{L}_2 -norm of Δ , *i.e.*,

$$\|\Delta_T\|_{\mathcal{L}_2} = \sqrt{\int_0^T \Delta^2 d\tau},$$

instead of the \mathcal{L}_2 -norm itself. The evolution of $\|\Delta_T\|_{\mathcal{L}_2}$ is plotted in Fig. 4. As one would expect, it increases significantly shortly after the disturbance and settles once the transients in f_{av} and $P_{\text{PFC,tot}}$ have decayed. The magnitude of $\|\Delta_T\|_{\mathcal{L}_2}$ can be shaped by varying the magnitude of the delay d in the DREM operator $[\mathcal{H}(\cdot)](t) = (\cdot)(t-d)$, see (11). In our experience, the best results can be obtained with $d \in [1, 8]$ s, which—as mentioned above—also roughly corresponds to the time span during which the inertia constant has the strongest influence on the aggregated power system trajectories, see also Fig. 2a.

TABLE II: Overview of estimator performance in different test cases

Test case	$P_{\text{PFC,tot}}$ obtained...	Estimation error
1: Outage SG at bus 645	... directly	$\max_{i=1,2} \left \frac{\eta_i - \hat{\eta}_i^s}{\eta_i} \right = 0.01$
	... via (20)	$\max_{i=1,2} \left \frac{\eta_i - \hat{\eta}_i^s}{\eta_i} \right = 0.07$
2: Outage SG at bus 644	... directly	$\max_{i=1,2} \left \frac{\eta_i - \hat{\eta}_i^s}{\eta_i} \right = 0.02$
	... via (20)	$\max_{i=1,2} \left \frac{\eta_i - \hat{\eta}_i^s}{\eta_i} \right = 0.07$
3: Rescheduling	... directly	$e_{\text{avg}} = 0.08$, see (21)

V. FURTHER TEST CASES: GENERATOR OUTAGE AND RESCHEDULING

The performance and accuracy of the inertia estimator (17) is investigated via further test scenarios. The same ENTSO-E system and simulation software as well as the same estimator tuning gains as detailed in Section IV are employed. The latter is crucial to assess whether a single set of tuning gains yields satisfactorily performances in diverse operating scenarios.

A. Online-Inertia Estimation: Further Generator Outage

To confirm the positive results of the previous section, we investigate the estimator performance in another generator outage scenario. In this second test scenario the PFC unit ‘ES917736’ in Spain with $S_{B_{644}} = 1227$ MW and $P_{m,644} = 1013$ MW is tripped. For this scenario we obtain a stationary estimation error of 7%, which is reduced to 2% if the measurement of $P_{\text{PFC,tot}}$ is directly taken from the simulation in RAMSES as input to the estimator, instead of using the model (20). Hence, despite the fact the generators are in different countries in each scenario, the obtained results are very similar to those of the previous scenario investigated in Section IV. An overview of the obtained estimator performance in different scenarios is given in Table II.

B. Online-Inertia Estimation: Rescheduling Events

As discussed in Section IV, a certain level of variation of the measurement signal(s), also referred to as excitation in the parameter identification literature [22]–[24], is essential for the estimation problem to be feasible. The frequency variation under usual operating conditions does—in our experience—not possess a sufficient level of excitation. Therefore, thus far and in line with other online inertia estimation approaches [13], [14], we have focused our performance analysis on outage scenarios. While these are clear opportunities for inertia estimation, their occurrence is rather infrequent and unscheduled. Hence, the question arises whether there are other operating scenarios, which can be exploited to perform the estimation.

In this context, imbalances resulting from scheduling changes can lead to significant frequency variations [28]–[30]. In particular, this applies to rescheduling events at full hours [28]–[30]. Hence, these are frequent, recurring, and scheduled frequency variations, which can be another useful source for inertia estimation.

A typical frequency evolution during a rescheduling process is shown in Fig. 5. This exemplary frequency trajectory f_{av} is

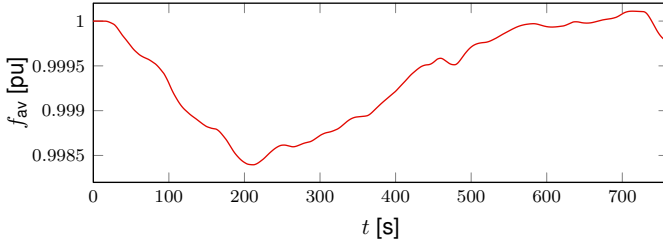


Fig. 5: Typical evolution of the (average) system frequency during a rescheduling process, based on [28, Fig. 1.2].

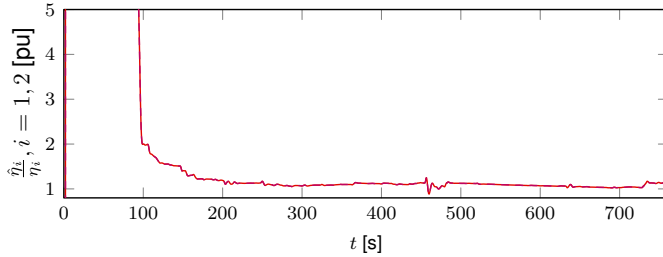


Fig. 6: Trajectories of the parameter estimates $\hat{\eta}$ relative to the nominal parameter values η , *i.e.*, $\frac{\hat{\eta}_i}{\eta_i}$ ($i = 1$ ‘-’ and $i = 2$ ‘-’) with initial condition $\hat{\eta}(0) = \text{diag}(0.3, 0.2)\eta$ in the rescheduling scenario.

based on [28, Fig. 1.2] and has been reproduced in RAMSES using the ENTSO-E system described in Section IV and performing scheduled power setpoint changes to generators and loads. Furthermore, we measure $P_{\text{PFC,tot}}$ directly from the simulation results in RAMSES. Feeding both signals f_{av} and $P_{\text{PFC,tot}}$ to the estimator (17) yields the relative estimation trajectories $\frac{\hat{\eta}_i}{\eta_i}$, $i = 1, 2$, shown in Fig. 6. It can be seen that the trajectories converge to a band around the nominal value of 1. Due to the continuous variations in the estimator input signals—indicating a non-stationary behavior of the whole system—also the parameter estimates do not converge to constant values. However, we find that the maximum average relative estimation error e_{avg} over the time window $t \in [T_1, T_2] = [300, 761]\text{s}$ is given by

$$e_{\text{avg}} = \max_{i=1,2} \left(\frac{1}{T_2 - T_1} \int_{T_1}^{T_2} \left| \frac{\eta_i - \hat{\eta}_i(\tau)}{\eta_i} \right| d\tau \right) = 0.08. \quad (21)$$

Hence, also in this scenario, the estimation error is below 10%. This confirms both that rescheduling events can provide useful data for inertia estimation and that the proposed DREM-based estimator (17) is well-suited for this task.

Remark 5.1: In the rescheduling scenario the variations in the generator power injection are not solely dictated by the model (20), but also by the rescheduling sequences, *i.e.*,

$$\Delta P = P_{m,\text{PFC}} + P_{\text{PFC,tot}} + P_{\text{res,PFC}} - P_{e,\text{PFC}},$$

where $P_{\text{res,PFC}} : \mathbb{R}_{\geq 0} \rightarrow \mathbb{R}_{\geq 0}$ denotes the power variation of the PFC units due to the rescheduling event. Therefore in this scenario using the model (20) does not yield any significant advantages and is thus omitted.

VI. CONCLUSIONS

An algorithm to monitor in real time the inertia constant of a large-scale power system has been presented. The increasing penetration of renewable energy units makes this a highly desirable feature to gain a better understanding of the system’s inertial frequency response and the security of the system in near to real time. In addition to the inertia constant, the aggregated mechanical power setpoint of the PFC generators is also estimated.

The proposed estimator is based on a nonlinear, aggregated power system model and constructed using the recently proposed DREM procedure. Its performance has been demonstrated via several test scenarios, in all of which the estimation error was below 10%. Remarkably, our approach is also applicable in rescheduling events, which occur numerous times every day in any deregulated power system. This is a distinguished feature compared to other existing solutions and significantly enhances the applicability of our solution.

The proposed estimator opens the door for many subsequent applications in the realm of power system protection and real-time control. Exploring these possibilities will be part of our future research.

REFERENCES

- [1] A. Ulbig, T. S. Borsche, and G. Andersson, “Impact of low rotational inertia on power system stability and operation,” *IFAC Proceedings Volumes*, vol. 47, no. 3, pp. 7290–7297, 2014.
- [2] W. Winter, K. Elkington, G. Bareux, and J. Kostevc, “Pushing the limits: Europe’s new grid: Innovative tools to combat transmission bottlenecks and reduced inertia,” *IEEE Power and Energy Magazine*, vol. 13, no. 1, pp. 60–74, 2015.
- [3] E. Ørum, M. Kuivaniemi, M. Laasonen, A. I. Bruseth, E. A. Jansson, A. Danell, K. Elkington, and N. Modig, “Future system inertia,” *ENTSOE, Brussels, Tech. Rep.*, 2015.
- [4] F. Milano, F. Dörfler, G. Hug, D. J. Hill, and G. Verbič, “Foundations and challenges of low-inertia systems,” in *2018 Power Systems Computation Conference (PSCC)*. IEEE, 2018, pp. 1–25.
- [5] T. Inoue, H. Taniguchi, Y. Ikeguchi, and K. Yoshida, “Estimation of power system inertia constant and capacity of spinning-reserve support generators using measured frequency transients,” *IEEE Transactions on Power Systems*, vol. 12, no. 1, pp. 136–143, 1997.
- [6] D. P. Chassin, Z. Huang, M. K. Donnelly, C. Hassler, E. Ramirez, and C. Ray, “Estimation of WECC system inertia using observed frequency transients,” *IEEE Transactions on Power Systems*, vol. 20, no. 2, pp. 1190–1192, 2005.
- [7] P. M. Ashton, C. S. Saunders, G. A. Taylor, A. M. Carter, and M. E. Bradley, “Inertia estimation of the GB power system using synchrophasor measurements,” *IEEE Transactions on Power Systems*, vol. 30, no. 2, pp. 701–709, 2015.
- [8] D. Zografos and M. Ghandhari, “Power system inertia estimation by approaching load power change after a disturbance,” in *Power & Energy Society General Meeting, 2017 IEEE*. IEEE, 2017, pp. 1–5.
- [9] D. Zografos, M. Ghandhari, and K. Paridari, “Estimation of power system inertia using particle swarm optimization,” in *Intelligent System Application to Power Systems (ISAP), 2017 19th International Conference on*. IEEE, 2017, pp. 1–6.
- [10] D. Zografos, M. Ghandhari, and R. Eriksson, “Power system inertia estimation: Utilization of frequency and voltage response after a disturbance,” *Electric Power Systems Research*, vol. 161, pp. 52–60, 2018.
- [11] K. Tuttleberg, J. Kilter, D. H. Wilson, and K. Uhlen, “Estimation of power system inertia from ambient wide area measurements,” *IEEE Transactions on Power Systems*, 2018.
- [12] S. Guo and J. Bialek, “Synchronous machine inertia constants updating using wide area measurements,” in *Innovative Smart Grid Technologies (ISGT Europe), 2012 3rd IEEE PES International Conference and Exhibition on*. IEEE, 2012, pp. 1–7.

- [13] P. Wall, F. Gonzalez-Longatt, and V. Terzija, "Estimation of generator inertia available during a disturbance," in *Power and Energy Society General Meeting, 2012 IEEE*. Citeseer, 2012, pp. 1–8.
- [14] P. Wall, P. Regulski, Z. Rusidovic, and V. Terzija, "Inertia estimation using PMUs in a laboratory," in *Innovative Smart Grid Technologies Conference Europe (ISGT-Europe), 2014 IEEE PES*. IEEE, 2014, pp. 1–6.
- [15] X. Cao, B. Stephen, I. F. Abdulhadi, C. D. Booth, and G. M. Burt, "Switching Markov Gaussian models for dynamic power system inertia estimation," *IEEE Transactions on Power Systems*, vol. 31, no. 5, pp. 3394–3403, 2016.
- [16] J. Zhang and H. Xu, "Online identification of power system equivalent inertia constant," *IEEE Transactions on Industrial Electronics*, vol. 64, no. 10, pp. 8098–8107, 2017.
- [17] S. Aranovskiy, A. Bobtsov, R. Ortega, and A. Pyrkin, "Performance enhancement of parameter estimators via dynamic regressor extension and mixing," *IEEE Transactions on Automatic Control*, vol. 62, no. 7, pp. 3546–3550, 2017, see also [arXiv:1509.02763](https://arxiv.org/abs/1509.02763).
- [18] P. Aristidou, S. Lebeau, and T. Van Cutsem, "Power system dynamic simulations using a parallel two-level schur-complement decomposition," *IEEE Transactions on Power Systems*, vol. 31, no. 5, pp. 3984–3995, Sept 2016.
- [19] V. V. Terzija, G. Valverde, D. Cai, P. Regulski, V. Madani, J. Fitch, S. Skok, M. Begovic, and A. G. Phadke, "Wide-area monitoring, protection, and control of future electric power networks." *Proceedings of the IEEE*, vol. 99, no. 1, pp. 80–93, 2011.
- [20] G. Anderson, "Lecture notes in dynamics and control of electric power systems," February 2012.
- [21] J. Weckesser and T. van Cutsem, "An equivalent to represent inertial and primary frequency control effects of an external system," *IET Generation, Transmission & Distribution*, 2017.
- [22] S. Sastry and M. Bodson, *Adaptive control: stability, convergence and robustness*. Courier Corporation, 2011.
- [23] A. Astolfi, D. Karagiannis, and R. Ortega, *Nonlinear and adaptive control with applications*. Springer Science & Business Media, 2007.
- [24] K. S. Narendra and A. M. Annaswamy, *Stable adaptive systems*. Courier Corporation, 2012.
- [25] R. Ortega, L. Praly, S. Aranovskiy, B. Yi, and W. Zhang, "On dynamic regressor extension and mixing parameter estimators: Two Luenberger observers interpretations," *Automatica*, vol. 58, no. 8, 2018.
- [26] A. Semerow, S. Hhn, M. Luther, W. Sattinger, H. Abildgaard, A. D. Garcia, and G. Giannuzzi, "Dynamic study model for the interconnected power system of continental europe in different simulation tools," in *2015 IEEE Eindhoven PowerTech*, June 2015, pp. 1–6.
- [27] P. Pourbeik *et al.*, "Dynamic models for turbine-governors in power system studies," *IEEE Task Force on Turbine-Governor Modeling*, 2013.
- [28] T. Weißbach, "Verbesserung des kraftwerks-und netzregelverhaltens bezüglich handelsseitiger fahrplanänderungen," Ph.D. dissertation, University of Stuttgart, 2009.
- [29] T. Weißbach and E. Welfonder, "High frequency deviations within the european power system—origins and proposals for improvement," *VGB powertech*, vol. 89, no. 6, p. 26, 2009.
- [30] L. Hirth and I. Ziegenhagen, "Balancing power and variable renewables: Three links," *Renewable and Sustainable Energy Reviews*, vol. 50, pp. 1035–1051, 2015.



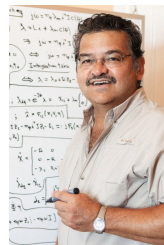
Johannes Schiffer received the Diploma degree in engineering cybernetics from the University of Stuttgart, Germany, in 2009 and the Ph.D. degree (Dr.-Ing.) in electrical engineering from Technische Universität (TU) Berlin, Germany, in 2015.

He currently holds the chair of Control Systems and Network Control Technology at Brandenburgische Technische Universität Cottbus-Senftenberg, Germany. Prior to that, he has held appointments as Lecturer (Assistant Professor) at the School of Electronic and Electrical Engineering, University of Leeds, U.K. and as Research Associate in the Control Systems Group and at the Chair of Sustainable Electric Networks and Sources of Energy both at TU Berlin.

In 2017 he and his co-workers received the Automatica Paper Prize over the years 2014–2016. His current research interests include distributed control and analysis of complex networks with application to microgrids and power systems.



Petros Aristidou (S'10-M'15) received a Diploma in Electrical and Computer Engineering from the National Technical University of Athens, Greece, in 2010, and a PhD in Engineering Sciences from the University of Liège, Belgium, in 2015. He is currently a Lecturer (Assistant Professor) in Smart Energy Systems at the University of Leeds, U.K. His research interests include power system dynamics, control, and simulation.



Romeo Ortega (S'81, M'85, SM'98, F'99) was born in Mexico. He obtained his BSc in Electrical and Mechanical Engineering from the National University of Mexico, Master of Engineering from Polytechnical Institute of Leningrad, USSR, and the Docteur D'Etat from the Polytechnical Institute of Grenoble, France in 1974, 1978 and 1984 respectively.

He then joined the National University of Mexico, where he worked until 1989. He was a Visiting Professor at the University of Illinois in 1987–88 and at the McGill University in 1991–1992, and a Fellow of the Japan Society for Promotion of Science in 1990–1991. He has been a member of the French National Researcher Council (CNRS) since June 1992. Currently he is in the Laboratoire de Signaux et Systemes (SUPELEC) in Gif-sur-Yvette. His research interests are in the fields of nonlinear and adaptive control, with special emphasis on applications.

Dr Ortega has published three books and more than 290 scientific papers in international journals, with an h-index of 79. He has supervised more than 30 PhD thesis. He has served as chairman in several IFAC and IEEE committees and participated in various editorial boards.